Ecological Informatics 81 (2024) 102612

Contents lists available at ScienceDirect

Ecological Informatics

journal homepage: www.elsevier.com/locate/ecolinf

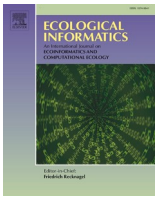

# Wildfire response of forest species from multispectral LiDAR data. A deep learning approach with synthetic data

Lino Comesaña-Cebral *, Joaquín Martínez-Sánchez, Gabriel Suárez-Fernández, Pedro Arias

*CINTECX, Universidade de Vigo, Applied Geotechnology Group, 36310 Vigo, Spain*

ARTICLE INFO

*Keywords:*
Multispectral LiDAR
Deep learning
Fire response
Synthetic data
Wildfire

ABSTRACT

Forests play a crucial role as the lungs and life-support system of our planet, harbouring 80% of the Earth's biodiversity. However, we are witnessing an average loss of 480 ha of forest every hour because of destructive wildfires spreading across the globe. To effectively mitigate the threat of wildfires, it is crucial to devise precise and dependable approaches for forecasting fire dynamics and formulating efficient fire management strategies, such as the utilisation of fuel models.

The objective of this study was to enhance forest fuel classification that considers only structural information, such as the Prometheus model, by integrating data on the fire responses of various tree species and other vegetation elements, such as ground litter and shrubs. This distinction can be achieved using multispectral (MS) Light Detection and Ranging (LiDAR) data in mixed forests. The methodology involves a novel approach in semantic classifications of forests by generating synthetic data with semantic labels regarding fire responses and reflectance information at different spectral bands, as a real MS scanner device would detect. Forests, which are highly intricate environments, present challenges in accurately classifying point clouds. To address this complexity, a deep learning (DL) model for semantic classification was trained on synthetic point clouds in different formats to achieve the best performance when leveraging MS data.

Forest plots in the study region were scanned using different Terrestrial Laser Scanning sensors at wavelengths of 905 and 1550 nm. Subsequently, an interpolation process was applied to generate the MS point clouds of each plot, and the trained DL model was applied to classify them. These classifications surpassed the average thresholds of 90% and 75% for accuracy and intersection over union, respectively, resulting in a more precise categorisation of fuel models based on the distinct responses of forest elements to fire. The results of this study reveal the potential of MS LiDAR data and DL classification models for improving fuel model retrieval in forest ecosystems and enhancing wildfire management efforts.

## 1. Introduction

Forests are among the most important ecosystems on Earth and provide a wide range of ecological, economic, and social benefits (Baciu et al., 2021). They are home to a variety of plant and animal species and are crucial in regulating global climate by absorbing carbon dioxide from the atmosphere (Azizi et al., 2023). Forests also provide numerous economic benefits such as timber, non-timber forest products, and recreational opportunities for tourism and outdoor activities (Ramakrishnan, 2007).

However, forest ecosystems are becoming increasingly vulnerable to wildfires that can cause significant damage to natural resources and human communities (Sullivan and Sullivan, 2016). Wildfires have severe ecological effects, including habitat destruction, biodiversity loss, soil erosion, and nutrient depletion (Geraskina et al., 2022). They can also have devastating economic and social consequences such as property damage, loss of income, and loss of life (Çolak and Sunar, 2020).

To manage the risk of wildfires, it is essential to develop accurate and reliable methods for predicting fire behaviour and developing effective fire-management strategies (Daşdemir et al., 2021). A critical component of this effort is the development of fuel models that provide information on the composition, structure, and distribution of forest fuels (Ferster and Coops, 2016). Fuel models are used to estimate the rate and intensity of fire spread and the heat release and fuel consumption associated with a wildfire (Xu et al., 2022).

Traditionally, fuel models have been developed using field-based

* Corresponding author.
*E-mail address:* linojose.comesana@uvigo.gal (L. Comesaña-Cebral).

https://doi.org/10.1016/j.ecoinf.2024.102612
Received 18 September 2023; Received in revised form 19 April 2024; Accepted 20 April 2024
Available online 22 April 2024

data collection and manual interpretation (Xu et al., 2022). This approach involves sampling and measuring forest fuels in the field, and then extrapolating the results to the entire forested landscape. Although this method provides accurate and reliable fuel models, it is time-consuming, labour-intensive, and expensive (Arroyo et al., 2008).

Recent studies have focused on using remote sensing data such as radio detection and ranging (RADAR), multispectral (MS) imagery, and Light Detection and Ranging (LiDAR) data to estimate forest fuel models (Labenski et al., 2022). These models can be categorised based on the technologies employed (active or passive sensors).

Passive sensors, which use MS images, cover a broad spectral range, facilitating species identification and fuel classification (Abdollahi and Yebra, 2023). However, these sensors lack penetration through the canopy cover, making them unsuitable for characterising the forest fuel structure and understory vegetation composition (Mihajlovski et al., 2023). Additionally, the restricted spatial resolution limits the precision of fuel classifications. For instance, Labenski et al. (2022) employed MS images at the plot scale to retrieve surface fuel models, resulting in scale-dependent outcomes due to the challenge of discerning small ground features. Another example can be found in Bjånes et al. (2021), in which the authors used satellite imagery data for 15 fire-influencing factors and trained different deep learning (DL) models to generate accurate wildfire susceptibility maps. Similar approaches were used in Sivrikaya et al. (2024) and Van Le et al. (2021), where four vegetation indices and a simple three-layered DL model were used to predict forest fire susceptibility maps on MS images from the Landsat-8 OLI.

Active microwave data present another option for evaluating vegetation height, biomass, and forest structure by employing techniques such as RADAR and interferometric synthetic aperture radar (Lavalle and Khun, 2014). These methods provide valuable insights into fuel type classification, as evidenced by Abdollahi and Yebra (2023). For instance, Mihajlovski et al. (2023) utilised a combination of multi-sourced data, including airborne laser scanning (ALS), MS imagery, and RADAR data, to assess fuel models in forest environments.

In addition, some studies have explored the use of active sensors alone for fuel modelling, such as those based on the LiDAR technology. For example, Botequim et al. (2019) used LiDAR data to describe how canopy fuel characteristics and spatial fire simulation can improve fire behaviour models for Mediterranean forests. They concluded that the weakest relationships were found in mixed forests, where the fuel loading variability was the highest. Furthermore, González-Ferreiro et al. (2014) used very low-density airborne LiDAR data to estimate canopy fuel characteristics in northwestern Spain. They found that the LiDAR-derived metrics and field-based fuels were strongly correlated. However, translating parameters derived from LiDAR data into fuel models necessitates precise characterisation of the vegetation structure, which may pose challenges depending on the fuel classification system employed (Marino et al., 2016).

Conversely, the combination of passive and active sensors aids in discerning the vertical vegetation structure, which explains the widespread use of MS imagery-LiDAR data fusion techniques (Lian et al., 2022). One example is Erdody and Moskal (2010), in which MS imagery and LiDAR data were fused to classify forest canopy fuels in the Ahtanum State Forest, USA. In addition, D'Este et al. (2021) used a fusion of multi-source remote sensing data, such as MS imagery and LiDAR data, to estimate the fine dead fuel load in the Apulia Region, Italy. Different algorithms have been used, such as the Support Vector Machine (SVM) and Random Forest (RF). Furthermore, Torresani et al. (2023) used Lang10m data, which comprised canopy height models (CHMs) derived from the fusion of recently published LiDAR Global Ecosystem Dynamics Investigation (GEDI) data and Sentinel-2 images using a deep convolutional neural network (NN). The main objective of this study was to estimate forest tree heterogeneity and related tree species diversity in forest ecosystems using a combination of MS imagery and CHMs derived from GEDI LiDAR data. Additionally, Padalia et al. (2023) used GEDI footprints with in-situ, optical, and RADAR data to estimate forest aboveground biomass (AGB) using a RF-based algorithm. Notably, Guo et al. (2023) used a combination of multi-sourced data, such as field sampling, CHMs derived from GEDI LiDAR, terrain, and Sentinel data, to estimate forest CHM and AGB. As stated in subsequent sections, these studies are interesting within the context of the current study because data collected exclusively from hypothetical MS LiDAR devices are used to perform similar analyses, but from a terrestrial perspective, where it is easier to distinguish AGB features while lowering canopy mean height quality.

Integrating MS LiDAR data has shown great potential in improving fuel model retrieval by providing high-resolution data on forest structure and composition (Stefanidou et al., 2020). MS LiDAR combines traditional 3D LiDAR data to capture additional spectral information that can be used to identify and classify different types of forest vegetation. This additional information can be used to create more accurate and detailed fuel models, which can significantly improve wildfire management (Stefanidou et al., 2020) and improve forest fire management strategies. Overall, MS data can be a valuable tool for estimating forest fuel models and can significantly improve forest fire management strategies.

However, there is still room for improvement, particularly in terms of classification algorithms. As described in the literature, traditional pixel-based machine learning techniques, including NNs and SVMs, have been widely employed for fuel-type classification in MS imagery data. These approaches assume independence among individual pixels and neglect their spatial interactions with neighbouring pixels during processing (Cleve et al., 2008). Object-based image analysis (OBIA) is another prevalent approach that stands out for its integration of diverse information, including textural, spatial, and spectral data, through multiscale image segmentation, leading to significantly improved accuracy (Alonso-Benito et al., 2016). However, the application of OBIA is intricate and demanding, owing to the necessity for various input variables. Moreover, two prominent challenges persist throughout OBIA: determining a suitable scale for image segmentation, and selecting appropriate features for image classification (Abdollahi and Yebra, 2023).

Moreover, enhancements in the classification outcomes of fuel types can be achieved using advanced DL classification models that can better handle complex and high-dimensional data from MS geoinformation such as LiDAR point clouds or MS imagery. DL is a subfield of machine learning that uses Artificial NNs to learn from large datasets and make accurate predictions using new data (Sharma et al., 2021). The ability of DL models to learn complex patterns and relationships in data makes them particularly well-suited for fuel model retrieval, where there are often many variables and relationships to consider, such as the horizontal and vertical continuities of different vegetal species (Skowronski et al., 2007). For instance, Kalinaki et al. (2023) used DL models such as U-Net and Deeplabv3+, to semantically classify forest and non-forest features using Sentinel-2 MS imagery. In addition, Marjani et al. (2023) used convolutional and recurrent NNs to analyse the spatial and temporal aspects of wildfires using MS imagery and Moderate Resolution Imaging Spectroradiometer data, which allowed the analysis of wildfire behaviour directly influenced by environmental parameters. Lin et al. (2024) used hyperspectral imagery to train three DL models (VGG19, ResNet50, and a combined version of these two), and different classifications of forest types were obtained regarding their representative tree species.

The use of DL classification models has emerged as a promising approach for automating fuel model retrieval from various sources of remote sensing data (Labenski et al., 2022). However, most studies within this context, whose methodologies involve mapping forest fuel characteristics, rely on image-based DL techniques, resulting in a significant gap in the application of more sophisticated models that utilise only LiDAR data as input. Point-cloud semantic segmentation using DL models has become a popular research topic in recent years owing to its applicability in various fields, such as autonomous driving, robotics, and

urban planning. Different methods have been proposed for this task, each with its own advantages and limitations. They can be grouped into three categories: projection-based, discretisation-based, and point-wise methods (Guo et al., 2021).

Projection-based methods project a point cloud onto one or more 2D planes and perform image-based semantic segmentation using convolutional NNs. This method leverages the success of 2D image segmentation methods and can be applied to point-cloud data. However, it suffers from information loss owing to the projection process and can be sensitive to the choice of projection direction and distance (Guo et al., 2021). Examples of these methods can be found in Fricker et al. (2019) and Hamraz et al. (2019) for the semantic classification of different tree species in forested environments.

Point-wise methods are the most straightforward approaches, where each point in the point cloud is considered an individual entity and is directly classified by a deep NN (DNN). Although this method can achieve high accuracy, it suffers from several issues such as the inability to capture the global context and inefficiency in processing large point clouds (Qi et al., 2017). Examples of these methods can be found in Xi et al. (2020) and Kaijaluoto et al. (2022) for forestry environmental characterisation.

Finally, discretization-based methods, divide the point cloud into a set of voxels or grids and treat each voxel as a unit of classification. This method can overcome the limitations of point-wise methods by capturing the global context and reducing computational cost. However, it suffers from a loss of information owing to the discretisation process and the limitation of the voxel resolution (Guo et al., 2021). Examples of these methods can be found in Wang et al. (2023) and Wang et al. (2021) for forestry environmental characterisation.

Regardless of the model type employed for semantic classification, training a DNN model from scratch requires a substantial number of training samples to grasp a diverse range of features. The lack of literature on semantic classifications of real LiDAR point clouds being pretrained with synthetic data emphasises the importance of integrating augmented data simulations during the training phase of DL models. Data augmentation addresses the requirement for large training datasets in DNNs, which can be achieved using an external simulator. Current research on LiDAR point-cloud simulations predominantly embraces two perspectives: aerial and terrestrial, specifically ALS, Terrestrial, and Mobile Laser Scanning (TLS and MLS, respectively) point clouds.

To the best of our knowledge, contemporary ALS simulators rely on the physical attributes of the laser beam, the target surface reflectance properties, and the trajectory geometry in a 3D virtual world. The approaches range from considering the laser as an infinitesimal beam with zero divergence to more intricate simulations involving full-waveform laser scanners. Kukko and Hyyppä (2009) introduced a sophisticated LiDAR simulator that accommodates various viewpoints, including TLS and MLS, with comprehensive consideration of laser physics in the forestry context. Kim et al. (2009) extended this method using radiometric simulations and clear 3D object representations.

Finally, TLS simulations cater to diverse needs, as evidenced by Wang et al. (2013), who employed a simplified model without beam divergence for leaf area index inversion. Conversely, Hodge (2010) detailed beam-divergence modelling and complete backscattered waveform simulations for TLS measurement error quantification.

Regarding the point-cloud simulation, the relevance of the HELIOS simulator presented in Bechtold and Höfle (2016) and, specifically, its enhanced version HELIOS++ (Winiwarter et al., 2022) are notable. With this openly accessible simulator, which can perform Virtual Laser Scanning from aerial and terrestrial perspectives, users can adjust simulations by blending various scales within a scene; for example, in the case of interest in the current study, modelling simultaneously detailed characteristics of trees with a voxel representation of the forest. HELIOS++ has such high usability that it allows the development of automated workflows, unlike most previously mentioned simulators.

To the best of our knowledge, there are no state-of-the-art studies on the employment of LiDAR point-cloud simulators to perform forest fuel estimation and analysis, highlighting another pioneering aspect of this study.

Precise fuel models in forests rely heavily on inventories that accurately represent the surrounding environment. Moreover, even if the two plots have similar geometric structures, resulting in the same fuel-type classification, these plots may respond differently to fire because of the distinct properties of the species. In other words, the varied responses of individual elements to fire could lead to the burning of specific plots at different rates and intensities. This highlights the rationale behind enhancing certain fuel models, such as Prometheus, which rely solely on structural information by incorporating semantic details regarding the fire response of each individual element in the inventory.

This study is unique because it introduces an innovative method for retrieving forest fuel models using MS LiDAR data and DL segmentation models. The main goal was to improve the established forest fuel models by incorporating further insights into the characteristics of vegetation species within mixed forests while adhering to the geometrical criteria set by the Prometheus model. Such valuable information can be accessed through MS data. Therefore, this novel methodology involves the exclusive employment of LiDAR point clouds interpolated at two different spectral bands as a single input. This demonstrates a departure from the norm observed in other state-of-the-art studies, where different combinations of multi-sourced remote sensing techniques are required, such as MS imagery and raw LiDAR point clouds. Furthermore, this study represents the first instance in the literature where a projection-based DL model was utilised to directly retrieve a forest inventory regarding the response to fire of the different species present in the case study. Among the novelties of this study, it is worth mentioning a pioneering aspect that involves the introduction of an MS 3D scene simulation for inventory tasks, generating labelled MS point clouds of forest environments that are suitable for feeding emerging DL models.

This paper is organised as follows: Section 2 presents the case study and methodologies of point-cloud generation, segmentation, and fuel type retrievals; Section 3 presents the different results achieved with different configurations of the DNN model with the resulting fuel type classifications; Section 4 discusses the previous results and compares them with similar methodologies in the literature; and Section 5 presents the conclusions.

## 2. Methodology

The workflow of this study is illustrated in Fig. 1. As a concise overview of the subsequent subsections, the methodology is structured as follows: first, the synthetic generator backbone and its utilities are explained; then, a state-of-the-art DL model is trained with the previously obtained synthetic data; and finally, a fuel-type classification is retrieved per MS cloud that was segmented by the DL model.

### 2.1. MS Forest point-cloud acquisition: case study

The first step of the proposed methodology involves collecting forest LiDAR data from different spectral bands. This is required to generate MS point clouds, which is performed by interpolating point clouds at different spectral bands. Synthesis of MS point clouds is required to fit three purposes:

- Input data to improve the synthetic generator (Section 2.2).
- Generating ground truth data for further validations (Section 2.3).
- Performing real-case inferences with the trained DL model (Section 2.4).

The TLS data were acquired from the Spanish region of O Xurés, Galicia (Fig. 2). It falls within the Baixa Limia-Serra do Xurés Natural Park, which has been designated as a region of special conservation (Novo et al., 2020). Plant life in the park is characterised by a deciduous

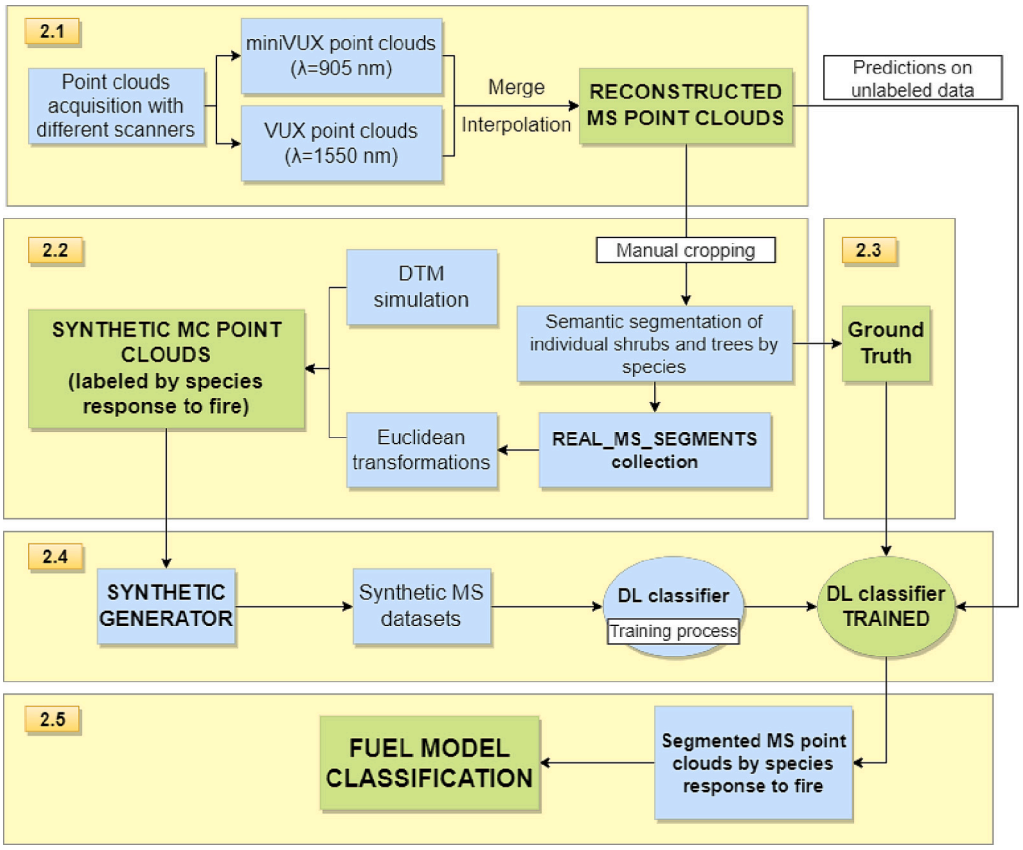


**Fig. 1.** Workflow of the method presented in this study. Numbers within the orange squares indicate the corresponding section.

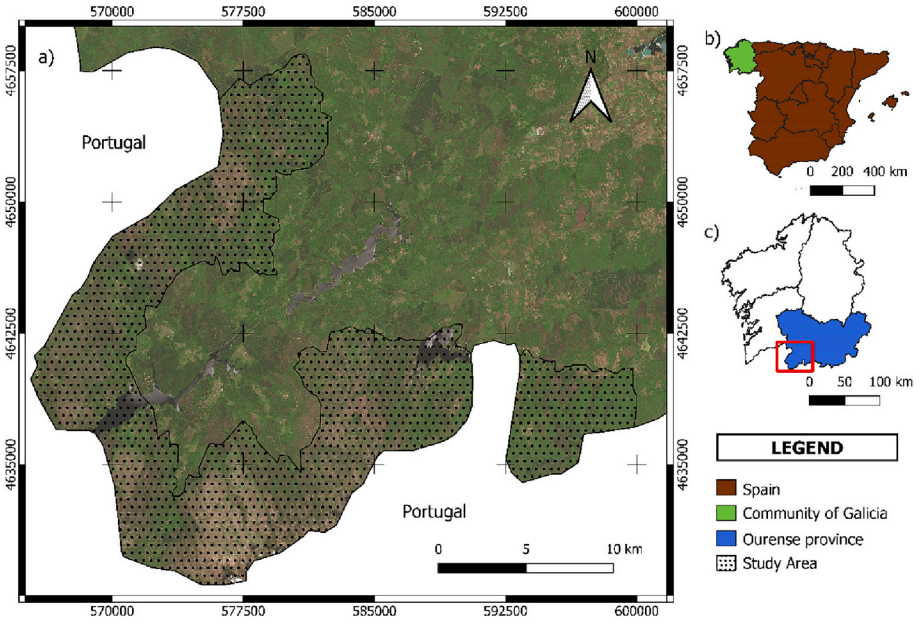


**Fig. 2.** Location of study area at different scales: (a) Region of O Xurés (Galicia, Spain), (b) location of the study area in Spain; (c) location of the study area in the province of Ourense.

forest comprising various tree species, such as *Quercus pyrenaica*, *Betula alba*, *Quercus suber*, *Arbustus unedo*, *Sorbus aucuparia*, and *Ilex aquifolium*. In addition to these species, there are several other endemic plants, including the Portuguese laurel and *Prunus lusitanica* (Novo et al., 2020).

TLS acquisition was performed using two different sensors mounted on a backpack, namely a Riegl VUX-1UAV and Riegl miniVUX-1DL (subsequently referred to as VUX and miniVUX, respectively). The detailed information and technical specifications of each sensor are listed in Table 1.

Because the same physical reality was scanned using different sensors, the geometry of the final MS scene was the union of all points in the VUX and miniVUX sets. However, the spectral information is incomplete

**Table 1**
Technical characteristics of the laser scanning systems (RIEGL MiniVUX-1DL Data Sheet, 2020)(RIEGL VUX-1UAV Data Sheet., 2020).

| Sensor | miniVUX-1DL | VUX-1UAV |
|---|---|---|
| Field of view | 46° ± 23° off-nadir | 330° |
| Scanning pattern | Circular | Linear |
| Pulse repetition frequency | 100 kHz | 550 kHz |
| Wavelength | 905 nm (NIR) | 1550 nm |
| Beam divergence | 1.6 × 0.5 mrad | 0.5 mrad |
| Footprint size at 100 m | 160 × 50 mm | 50 mm |
| Accuracy | 15 mm at 50 m | 10 mm at 150 m |
| Precision | 10 mm at 50 m | 5 mm at 150 m |

because each point has only one pair of (R, I) information points, where R and I are the reflectance and intensity values, respectively, and the remaining pair should be simulated. One way to overcome this issue is by applying the NN-interpolation method to the VUX and miniVUX sets, where the resulting point cloud is created by the union of both geometries, and each point has its original (R, I) pair and the (R, I) pair interpolated from its nearest neighbours in the complementary set.

### 2.2. Generation of synthetic MS point clouds

The aim of this synthetic generator is to simulate labelled and realistic MS forest point clouds fed to the DL-based classifier during the learning process. To do so, the simulator developed by Comesaña Cebral et al. (2022) was selected as the backbone and modified to include more field-site characteristics.

This simulator was created from scratch using DTM models that were subsequently filled with different semantic segments. Once both point clouds were merged into a unique MS point cloud, all elements of interest were identified, manually cropped from the scene, and stored in a new data collection called Real_MS_Segments. Examples of these elements, such as tree species, can be found in Fig. 3. This process is not limited to tree species; it also identifies crops, shrubs, and ground areas covered with litter and grass in the initial scene, and stores them in the Real_MS_Segments collection.

Finally, all components of the Real_MS_Segments were randomly positioned within the permissible areas of the DTM surface model while retaining their interpolated spectral information. In addition, because each point has a known origin in real MS point clouds, the points are labelled according to their semantic and instance information. Specifically, semantic details relate to the varied characteristics of vegetation species in response to fire. Although the criteria for assigning these attributes are explained in Section 2.5, these types of vegetation correspond to the following semantic classes: "fire-intolerant," "fire-retardant," and "fire-resistant" for tree segments and "fine-fuel" for shrubs segments and understorey areas. An illustration of these synthetic point clouds is shown in Fig. 4.

Finally, all these pipelines were unified within a single procedural framework, constituting an enhanced synthetic generator capable of synthesising several MS TLS forest point clouds, which were collected as a training dataset for the selected DL model (Section 2.4).

### 2.3. Ground truth labelling

The third step of the methodology was generating reliable ground truth data. This is required for Section 2.4, where a DL model is trained with the previously explained synthetic data, and its performance needs to be validated with real data to assess how well the model classifies MS forest point clouds.

The case study in this study consisted of different forest plots where different vegetation elements were present at different heights, making it difficult to segment them, even using a human classifier. Two examples of this behaviour can be seen in both subplots of Fig. 5, where multiple trees and shrubs are so close that it is difficult to see which point belongs to which element.

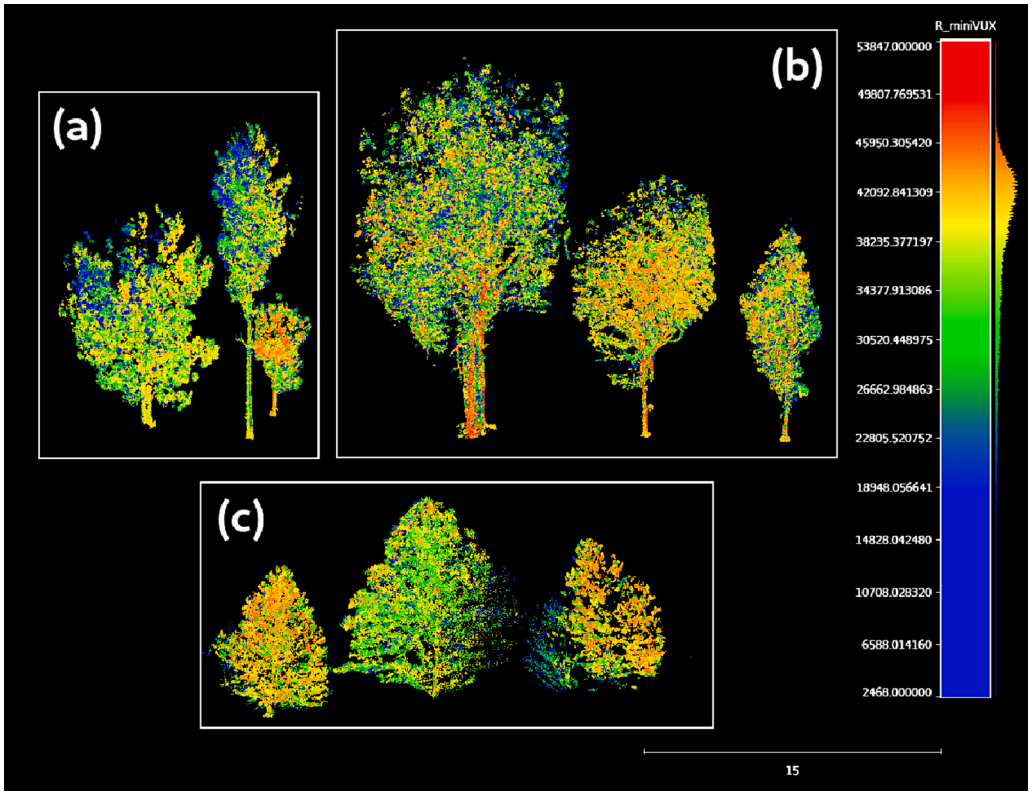


**Fig. 3.** Different MS samples of (a) *Pinus pinaster*, (b) *Quercus robur*, and (c) *Abies alba*, coloured by spectral reflectance at λ = 905 nm (miniVUX sensor operational band).

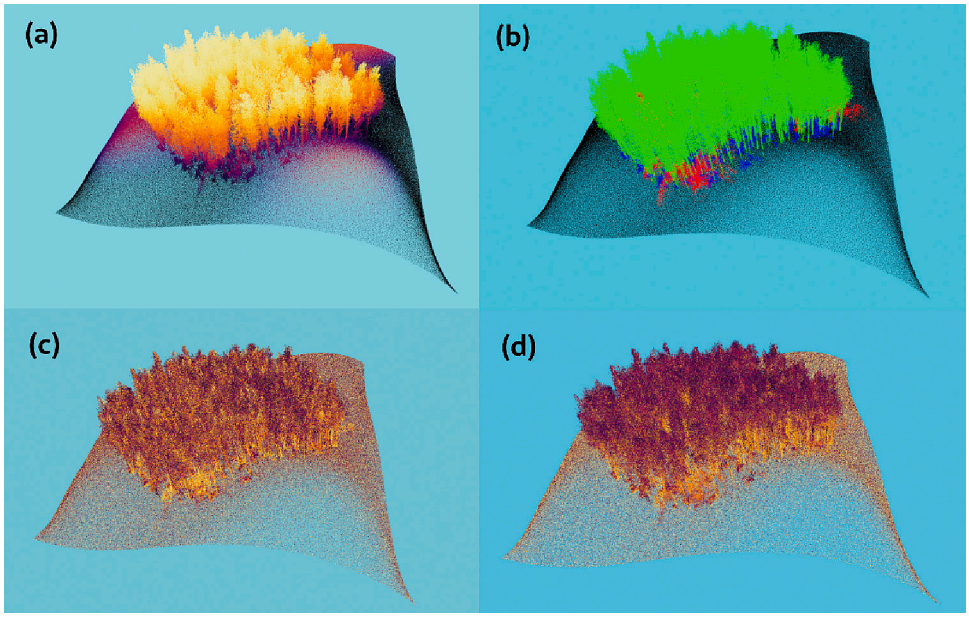


**Fig. 4.** Synthetic point-cloud example coloured by: (a) height, (b) semantic labels, (c) spectral reflectance at $\lambda = 905$ nm (miniVUX sensor band), and (d) spectral reflectance at $\lambda = 1550$ nm (VUX sensor band).

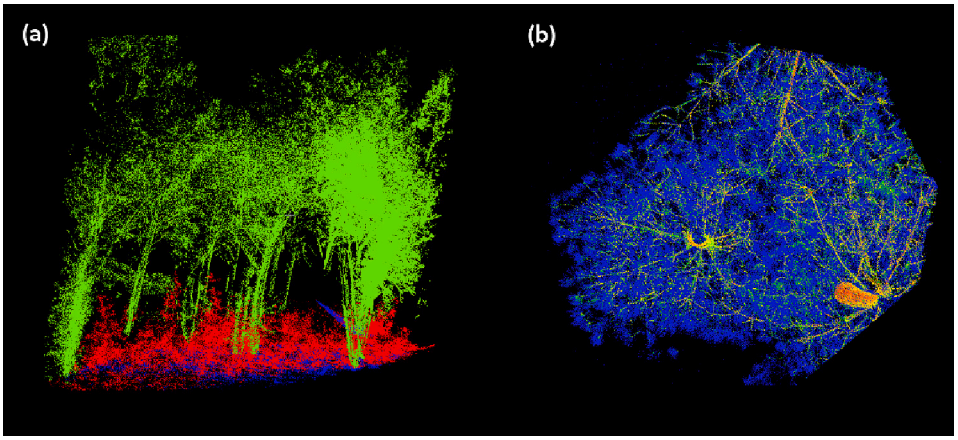


**Fig. 5.** (a) Trees (lime green) and shrubs (red). (b) Bottom view of tree crowns that are too close coloured by spectral reflectance at $\lambda = 905$ nm. (For interpretation of the references to colour in this figure legend, the reader is referred to the web version of this article.)

The objective of this section is to establish a reference for ground truth data, enabling the comparison of subsequent results using a hybrid methodology based on different algorithms, and minimising the error associated with the labelling process. The first approach involves filtering all points that belong to the ground and to the different shrubs and undergrowths present in the point cloud. Several state-of-the-art algorithms exist that suit the purpose of subtracting all points from the ground, such as those of Zhang et al. (2016) and Hui et al. (2016). Even if these methods were tested on ALS geometries, they also fit the purpose of the TLS point clouds. Moreover, the effectiveness can be improved in TLS scenarios because all points are acquired under the tree canopies; therefore, the ground points should be more reliable from this perspective than those taken from ALS devices, where the tree canopies can interfere and cause occlusions. Spectral reflectance information can help in the identification of shrubs and undergrowth because different components of the cloud have different spectral signatures, as shown in Fig. 6. For example, the wood from tree trunks and branches has a clearly differentiable reflectance range. Therefore, a reflectance filter in the range of $[-800, -100]$ is applied, and the resulting point cloud is combined again with the ground. In this new point cloud, it was easier to manually segment each shrub and undergrowth point.

The remaining points that were previously filtered were recombined with points labelled as ground, creating a new point cloud mostly composed of ground and tree points. Because the problem of retrieving single-tree information remains difficult, the algorithm developed by Comesaña-Cebral et al. (2021) was applied to obtain different clusters with individual and multiple trees. Because all forest plots present in the region mostly comprised *Pinus pinaster*, *Abies alba*, and *Quercus robur*, all points inside a cluster were classified according to the species of the tree or trees within it.

Although the method proposed in this section should be similar to the usual workflow in these cases and can be more precise than a manual labelling process, the amount of time and the requirement of a visual classification of the tree species make it recommended to develop an automatic method to segment point clouds in difficult environments such as thick woods.

### 2.4. Semantic segmentation with a DNN model

Once the generator presented in Section 2.2 can create synthetic MS

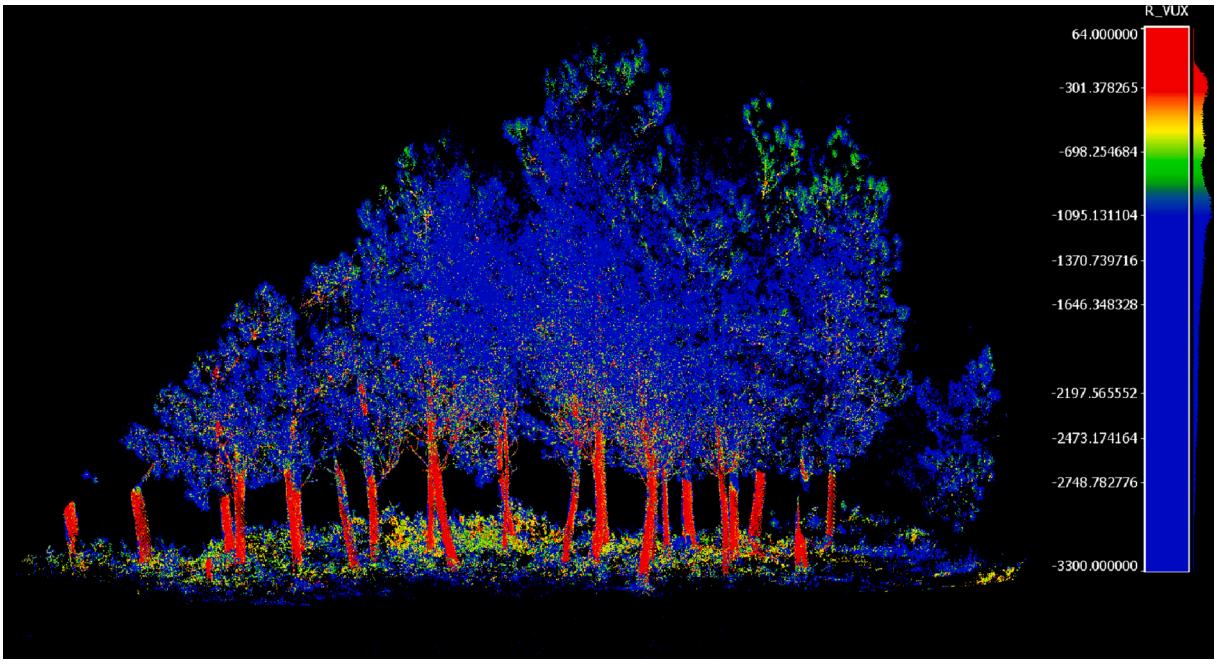


**Fig. 6.** Different elements within the forest inventory can be easily distinguished based on their spectral reflectance. For example, at $\lambda = 1550$ nm, tree trunks exhibit the highest reflectance, followed by shrubs and understorey, whereas tree crowns display lower reflectance levels.

TLS forest point clouds, as an initial step of this fourth block of the methodology, it is recursively utilised to collect a training dataset. Subsequently, a state-of-the-art DNN model called SoftGroup (Vu et al., 2022a) was selected and trained with this dataset to differentiate vegetation types regarding their response to fire within the MS LiDAR point clouds, as established by the assigned semantic classes.

The SoftGroup model was developed to segment point-cloud data; specifically, it performs a soft grouping technique over a set of points where semantic scores were previously retrieved. This model was selected based on its ability to efficiently process large-scale point clouds (Vu et al., 2022b), making it suitable for the scenarios described in this study. It demonstrated impressive performance on prominent datasets such as ScanNetV2 (Dai et al., 2017) and S3DIS (Armeni et al., 2016), further validating its effectiveness.

Because the fuel models that are going to be considered do not use individual information of single instances, this module will be limited to the semantic branch of the SoftGroup DNN model.

The NN takes a collection of N points as input, where each point is represented by its coordinates and two spectral reflectance values at distinct wavelengths, and outputs a vector with the indices of each point in the collection and another vector with their semantic scores. To facilitate further processing, the point set underwent voxelisation, transforming the points into sparse volumetric grids. These grids serve as the input for a U-Net-style backbone, enabling the extraction of point features.

Following the extraction of features from the backbone, inverse mapping of the voxelisation process was applied to recover the original point features. Subsequently, a semantic branch comprising a two-layer Multi-Layer Perceptron (MLP) was constructed. The MLP is trained to generate semantic scores, denoted as $S = \{S_1, \ldots, S_N\} \in R\ N \times N_{class}$, representing N points across $N_{class}$ different classes. Notably, the grouping of points was performed directly based on semantic scores without converting them into one-hot semantic predictions.

To assess the efficacy of the NN in semantic classification throughout the training, validation, and testing stages, we employed established quantitative metrics that are commonly used for image and 3D-scene segmentation (Everingham et al., 2015). These metrics include the Mean Accuracy (MA), MA Error (MAE), Intersection over Union (IoU), and Mean IoU (MIoU). Notably, in addition to the comprehensive evaluation provided by the Overall Accuracy and IoU, their mean counterparts (MA and MIoU) consider the individual values for each class within the dataset and compute their average. This approach enhances the reliability of the classification results for imbalanced data. Furthermore, the highest MIoU value was employed to determine the point at which the DNN attained optimal performance.

Finally, the selected SoftGroup architecture was trained over 1000 epochs for each type of input data, and metrics such as MIoU or MA were computed after each epoch to analyse the training performance. Once trained, the configuration weights that achieved the best classification performance were selected to establish the reference trained model and, finally, it was used to perform predictions on the real MS point clouds collected in Section 2.3, i.e. the ground truth data.

### 2.5. Fuel model retrieval

The fifth and final step of the proposed methodology involves determining which type of fuel model corresponds to the previously classified MS point clouds by considering the vegetation structure and species response to fire. Nonetheless, regardless of the input data source, traditional fuel modelling approaches from most studies do not consider important information concerning the responses of different species to fire. As detailed below, this supposes an enhancement of existing fuel-type schemes such as the Prometheus model.

The Prometheus fuel classification system was developed as a means of adapting the Northern Forest Fire Laboratory classification to better suit the Mediterranean environment (Arroyo et al., 2008). This system aims to provide a more appropriate classification of the types of fuels found in Mediterranean ecosystems. The main criteria for classification in this system are the type and height of the propagation element, which is divided into three primary groups: grasses, shrubs, and ground litter (Mutlu et al., 2008). The fuel types are then described based on the spatial distribution of the three primary groups.

By accounting for fuel height and density, the fire behaviour can be modelled using the following seven fuel types based on the inventory of the segmented point clouds (Riaño et al., 2002):

**Land Fuel (fuel type 1):** This category encompasses agricultural and

herbaceous grasslands with thin and dry vegetation during summer. Because of their composition, fires in this category spread rapidly at low flame altitudes.

**Low-Lying Shrubs (fuel type 2):** This category includes grasslands, low-lying shrubs (30–60 cm), and a high percentage (30–40%) of herbs. It also comprises lumbered areas where remnants of the lumber still exist.

**Medium Shrubs (fuel type 3):** This category comprises medium to large-sized shrubs (0.60–2.0 m), with land coverage often exceeding 50%. Natural and artificially regenerated areas may also be included.

**Tall Shrubs (fuel type 4):** This category includes tall shrubs (>2.0 m) and areas consisting of young tree groves resulting from regeneration.

**Forest Areas with No Understory (fuel type 5):** This category comprises areas where undergrowth has been intentionally removed, either through controlled burning or mechanical or chemical methods. In this category, low-spread fires are the most common.

**Forest Areas with Medium Understory (fuel type 6):** This category includes forests in which the leafy part of the tree is much higher than the uppermost parts of the understory, which typically consists of low-lying shrubs. Fires in this category are characterised by low density, with varying intensities that can escalate into markedly larger fires under extreme climatic conditions.

**Forest Areas with High and Dense Understory (fuel type 7):** This category includes forests with high and dense undergrowth, where the distance between the leafy part of the tree and the understory is small, or there is a merging of the two. This category is highly prone to severe high-density fires.

However, the precision of the Prometheus classification may be unreliable and could vary depending on the fuel elements present, as they demonstrate distinct burning and fire propagation characteristics, regardless of the structural features. The Prometheus fuel model incorporates height and various propagation elements, allowing the classification of surface fuels, such as live and dead trees, shrubs, grasses, forbs, and downed dead woody debris fuels, into specific fuel types based on their structural characteristics. This implies that the two plots classified as fuel type 6, according to the Prometheus model, may exhibit distinct burning and fire propagation characteristics if they contain different surface fuel elements. The Prometheus model only distinguishes elements based on their geometric shapes and does not consider information related to their responses to fire.

The types of tree species present are among the crucial factors influencing the risk of fire spread. For instance, conifer-dominated forests, such as those with *Pinus* or *Abies*, may require adjustments to the fuel model owing to the unique characteristics of these tree types (Blauw et al., 2017). *Abies alba*, categorised as "fire-intolerant," possesses a relatively thin bark and exhibits low post-fire resilience (Frejaville et al., 2013; Tinner et al., 2000). *Quercus robur*, labelled "fire-retardant," displays high resistance to low-intensity fires but is sensitive to moderate intensity, resulting in foliage loss and bark failures (Dupire et al., 2019). Conversely, *Pinus pinaster*, identified as "fire-resistant," thrives in shrubland regions, showing remarkable adaptation to high-intensity fires and outcompeting other species of fire-prone shrublands (Richardson et al., 1990). However, variations in ground litter production among different tree species also influence fuel models and spread of fire in the forest understorey (Bufacchi et al., 2020).

The outcomes of this study highlight the crucial role of tree species identity in shaping fuel dynamics, emphasising the need to account for such factors when developing forest fuel models to accurately predict fire behaviour and enhance wildfire management efforts.

These findings highlight the importance of tree species identity in fuel dynamics and underscore the need to incorporate such factors when designing forest fuel models for precise fire behaviour prediction and improved wildfire management strategies. Consequently, the classifications obtained from the DNN will be categorised under the following semantic labels: "fire-intolerant," "fire-retardant," and "fire-resistant" for points that belong to a tree and "fine-fuel" for points that belong to shrubs and understorey.

## 3. Results

### 3.1. DNN performance

The effectiveness of the proposed approach was demonstrated through experiments on a straightforward dataset of synthetic forest point clouds, with the aim of demonstrating significant improvements in accuracy and efficiency compared with traditional methods.

A summary of the main results of this section and a comparison with the results obtained by related studies are presented in Table 2. All the results obtained in Figs. 7 and 8 were achieved by training and testing the model with the synthetic MS data generated in Section 2.2, whereas inferences on the real data are presented in the next section. In addition, the graphs obtained were smoothed to overcome variability.

In the next section, the classifications of the real point clouds will be made using the MS-trained model, because it was proven that the model in this last experiment outperformed the previous ones, and their fuel type classifications will be more reliable.

### 3.2. Fuel model retrieval

Once the DL model is trained, a few samples of real MS point clouds are segmented using the methodology exposed in Section 2.3 to create a ground truth. This ground truth was required to validate the classifications using a DL model trained with synthetic data. As mentioned in the previous section, the best classification performance of the SoftGroup semantic branch was achieved by the MS input data case; therefore, this pretrained model was used, and its efficiency was tested by inferring these real MS point clouds (Fig. 9). In addition, these inferences on real MS point clouds are taken as inputs for the decision tree scheme presented in Section 2.5, where the final fuel models are retrieved. The final fuel model classifications are summarised in Table 3.

## 4. Discussion

The case study essentially involved dense forested areas, where the different species mentioned in Section 2.1 are distributed. In addition, there are small regions where some *Abies alba* samples, which represent fire-intolerant species, can be found alongside other types of vegetation that are more resistant to wildfires. These elements have a notably heterogeneous height distribution, which is a relevant feature to consider when analysing fire spread at different forest height levels. Considering these characteristics of the study area, nine forest plots

**Table 2**
Performances of different DL models applied on forest point clouds. * States for other additional kernels.

| Model | Data | Training kernels | MA (%) | MIoU (%) |
|---|---|---|---|---|
| **SoftGroup** (Ours) | TLS | [X, Y, Z] | 80.5 | 50.9 |
| | | [X, Y, Z, $R_1$] | 86.1 | 59.7 |
| | | [X, Y, Z, $R_2$] | 87.5 | 63.2 |
| | | [X, Y, Z, $R_1$, $R_2$] | **90.2** | **76.7** |
| **LSSegNet3** (Kaijaluoto et al., 2022) | TLS | [X, Y, Z, $R_2$, *] | **93.1** | 80.1 |
| **DCNN** (Hamraz et al., 2019) | TLS + Raster | [X, Y, I] | 85.1 | – |
| **RandLA-NET** (Kaijaluoto et al., 2022) | TLS | [X, Y, Z, $R_2$, *] | 92.9 | 80.6 |
| **PointCNN** (Xi et al., 2020) | TLS | [X, Y, Z, I] | 83.4 | 61.3 |
| **DCNN** (Fricker et al., 2019) | ALS + aerial imagery | [X, Y, Colour, *] | 86.7 | – |

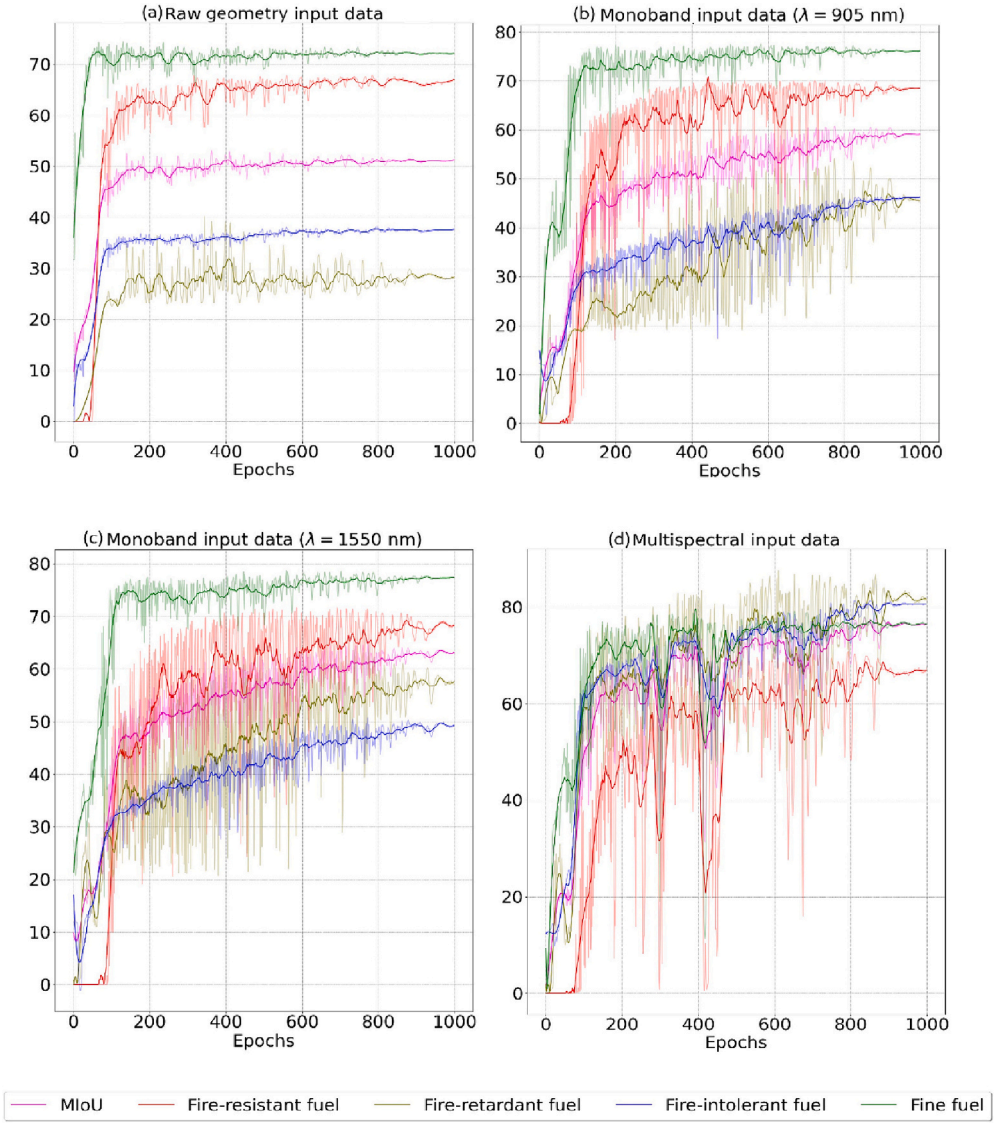


**Fig. 7.** MIoU and IoU values per class obtained during the training with point clouds in different formats as input data.

representing the heterogeneous aspects of the region were selected, and surveys with the two TLS mentioned in Table 1 were conducted. Because of the physical specifications of each scanner, the geometry detected differs in the spectral reflectance responses per point and in the spatial resolution, scale, and point density, leading to point clouds of ~5 M points (~50 MB per LAZ file) and ~ 40 M points (~500 MB per LAZ file) for the miniVUX-1DL and VUX-1UAV point clouds, respectively.

After the NN interpolation, the MS point clouds were retrieved for each of the nine plots. However, owing to computational limitations, these bulky point clouds pose a significant challenge to the accurate performance of DL models, whose layers cannot support such tensor sizes. Lowering the number of points in specific locations could lead to the loss of important information; however, a random downsampling process was applied to uniformly reduce the number of points while visually maintaining the forest structure. Furthermore, the aforementioned scanners provide more information that contributes to increase the size of the input tensors, such as the number of returns, amplitude, deviation, GPS time, and eco-deviation. Ideally, all these information fields would be helpful for the DL model to distinguish among the considered semantic classes. However, one of the crucial limitations facing all modern AI-based algorithms is their efficiency in terms of time and tensor allocation memory. Therefore, only spatial and spectral kernels were selected, and tensors with shapes [X, Y, Z, $R_1$, and $R_2$] were constructed to feed the SoftGroup model, as listed in Table 2. In addition, a system with four graphical processing units (NVIDIA A100 of 40 GB HBM2 memory) was used within the Finisterrae III Supercomputer node system of the Centro de Supercomputación de Galicia to address this limitation.

Concerning the generation of synthetic MS datasets, the pipeline introduced in Section 2.2 was applied to generate virtual data with spatial resolutions, scales, and point density similar to the real MS LiDAR that was previously interpolated. Five point clouds of 1 ha and 20 M points were simulated, consuming approximately 6 GB of memory in the process, similar to the ALS and TLS cases discussed in Winiwarter et al. (2022) regarding the HELIOS++ simulator, in which a system with an Intel-i9–7900 @ 3.3 GHz and 64 GB of RAM was used. The authors stated that each simulation was completed in <1 h; however, they argued that points concerning vegetation were obtained under voxel representations, hence lowering the level of detail, because environmental and climatic effects such as wind could hinder the simulation backend algorithms. In our case, it took approximately 24 min per simulated cloud, and it is important to mention that the proposed case of the study; hence, each synthetic scene consisted exclusively of forested areas, that is, there were only vegetation segments present in each scene.

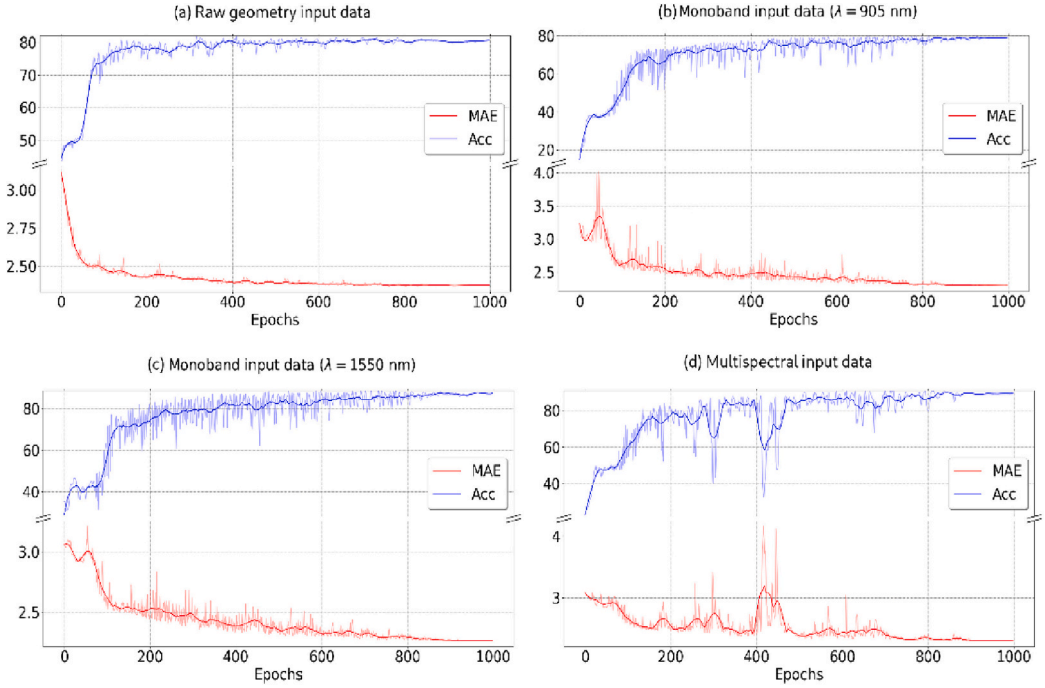


**Fig. 8.** Accuracies and MAE values obtained during the training with point clouds in different formats as input data.

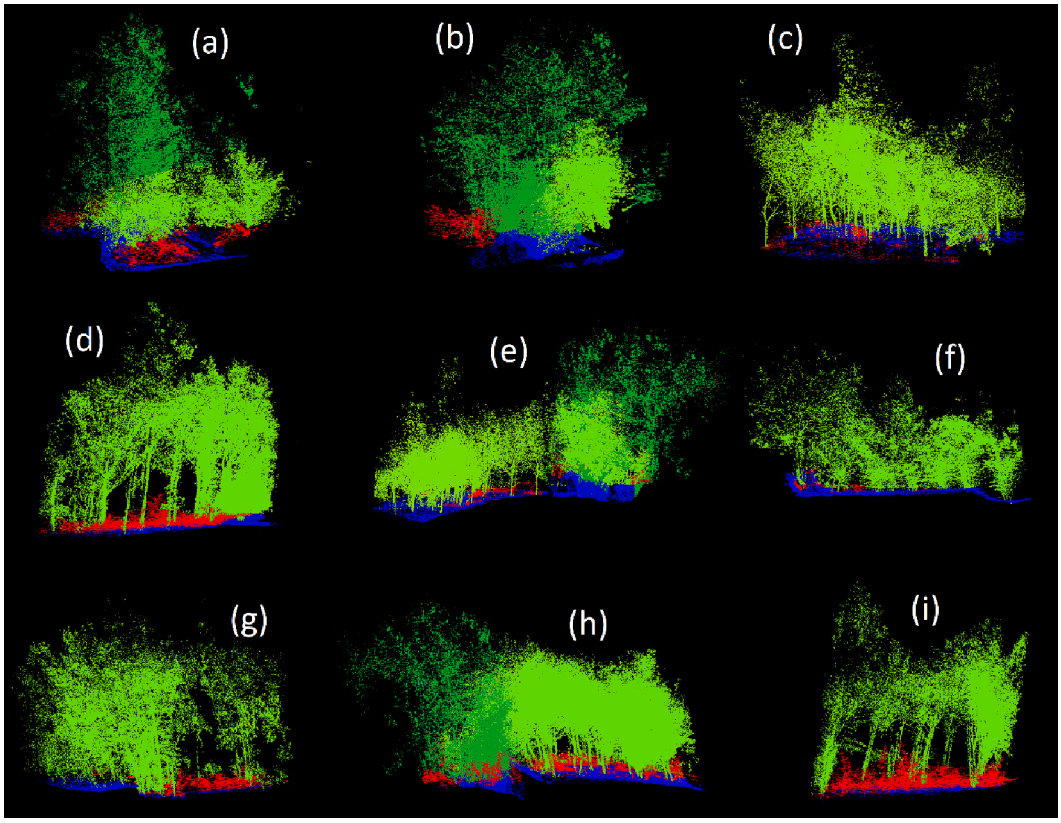


**Fig. 9.** Multispectral forest plots classified by the SoftGroup semantic branch. Dark green: fire-resistant, light green: fire-retardant, red: fine fuel, and blue: ground. (For interpretation of the references to colour in this figure legend, the reader is referred to the web version of this article.)

Consequently, the level of detail in point-cloud simulations remains important for ecological tasks such as fuel modelling and biomass analysis. In addition, the synthetic generator used in this study required only a previous collection of a few MS tree models, which were the most representative of each species, and the full 3D scene was automatically generated from scratch without user interaction. This is not the case for the HELIOS++ simulator which requires the specification of three main XML files as inputs concerning scanner properties, the platform that

**Table 3**
Prometheus fuel types obtained from the semantic classifications at different plots. Classes 0, 1, 2, and 3 denote fire-resistant, fire-retardant, fire-intolerant, and fine fuel, respectively.

| Plot index | IoU by classes | | | | MIoU | Fuel type | Abundance |
|---|---|---|---|---|---|---|---|
| | 0 | 1 | 2 | 3 | | | |
| 1 | 89.2 | – | 70.0 | 89.4 | 82.9 | 4 | Fire-intolerant |
| 2 | 82.6 | – | – | 63.5 | 73.1 | 5 | Fire-resistant |
| 3 | 82.7 | – | – | 62.3 | 72.5 | 6 | Fire-resistant |
| 4 | 72.5 | 75.5 | – | 45.3 | 64.4 | 5 | Mixed |
| 5 | 80.7 | 76.4 | – | 61.9 | 73.0 | 5 | Mixed |
| 6 | – | 86.5 | – | 51.2 | 68.9 | 6 | Fire-retardant |
| 7 | – | 89.7 | – | 59.8 | 74.8 | 5 | Fire-retardant |
| 8 | – | 92.8 | – | 49.5 | 71.2 | 5 | Fire-retardant |

carries the scanner, and the scene definition. Specifically, the last input was configured to manually design the scene and place each 3D object from an external collection, which supposes greater previous effort. However, the simulation process introduced in Section 2.2 does not consider any specific trajectory and physical characteristics of the scanner and does not perform any ray-tracing procedure such as HELIOS++, which is useful for non-ecological applications.

In <3 h, synthetic training and test datasets consisting of five and two point clouds, respectively, were simulated, and the SoftGroup DL model was fed into them. The different behaviours of the model are shown in Figs. 7 and 8. For example, in the graph (a) of Fig. 7, the model was trained exclusively with raw point clouds; that is, only the geometrical kernel was fed during training. This indicates that the number of features learned by the model was low, and convergence of the model was reached sooner than in the other experiments. This is reflected in the variability of each metric during training, which was clearly less noisy among all the experiments performed.

In graphs (b) and (c) of Fig. 7, the model was trained with monoband synthetic point clouds; thus, four kernels were fed: three geometrical and one spectral reflectance. Both behave in a common way, because there is no single fuel element that stands out from the others in one band but not in the other. Compared with the previous experiment, in which the model was fed only with raw point clouds, the improvement in the classifications was close to 10%. Xi et al. (2020) used different machine learning and DL methods to create a wood/nonwood classifier benchmark using point clouds with an intensity kernel as the input. Most DL models used projection-based examples, but PointCNN was also used, which is a point-wise-based model. The MIoU results obtained were close to 15% less than those achieved by the SoftGroup model used in this study.

Finally, in Fig. 7(d), the model was trained using the original MS synthetic data. Because some fuel elements are easier to identify in one band than in another and vice versa, the combination of the two bands considered in this study helps to better classify the forest fuel load. This is reflected by the fact that the MIoU score achieved by the model in this experiment was approximately 10% higher than both monoband highest scores, and close to 15% higher than the monoband cases of the work presented by Xi et al. (2020) and Hamraz et al. (2019). In addition, the convergence of the metrics appeared at an epoch similar to that in the previous experiments, around the 900th epoch. Kaijaluoto et al. (2022) trained three variations of a DL model, called LSSegNet, to classify forest point clouds into similar classes: ground, understorey, trunk, and foliage. Each variation differs from the others in terms of the number of convolutional layers and filters, and each variation is trained using input point clouds with different kernel configurations. The best results were achieved by the LSSegNet3 configuration with an 80.1% MIoU score, which is not significantly different from the 76.7% achieved in this study. However, this configuration only doubled the number of convolutional layers from the previous variations and increased the number of kernels used for the classifications; therefore, all the results can be grouped in the range of 74.7–80.1% of the MIoU score. Furthermore, Fricker et al. (2019) used a projection-based DL method to classify different tree species from hyperspectral images with 3D structural information from ALS data and their average results were in the order of ~4% less than the MS experiments done in this study.

The MIoU metrics in Table 3 vary from ~62% to ~83%, which are in the 60–80% range of the related work presented in Table 2 of the previous section. The main difference between the current study and previous ones is the use of synthetic data for training a DL model instead of a previous labelling process of real data, which can be highly time-consuming, even if it is performed manually by the user or by a traditional machine learning unsupervised method. The cases of plots 1 and 2, where the vegetation elements were easy to distinguish, resulted in high MIoU rates (up to ~83%), as shown in Fig. 10.

As shown in Table 2, there is an existing knowledge gap in the state-of-the-art methods concerning the DL-based segmentation of forest structures from raw geometry data in combination with other additional kernels, which are helpful in distinguishing features from similar 3D objects. Nevertheless, there are some advantages to using forest imagery that can also be extrapolated to studies concerning ALS and TLS measurements. For example, Kalinaki et al. (2023) employed two different DL models to classify the vegetation surrounding a highway and track its changes from satellite imagery. However, two classes were considered: forest and non-forest. Despite the scale of this case study, which reflects less resolution of small ground details, a wider characterisation of the vegetation could be performed by considering the various species present or differentiating types of vegetation regarding their surface cover, which are crucial to road management and wildfire ignition prevention. A different example can be found in Fricker et al. (2019), the study mentioned in the comparison in Table 2, where the authors used a projection-based DL model, which means that all information within the segmented images was interpolated to the original ALS point cloud. This approach is interesting from the historical perspective of the evolution from traditional to DL methodologies. However, even if the case study considers the combination of hyperspectral imagery with LiDAR point-cloud measurements, the same obstacle concerning the aerial perspective remains present, thereby reducing the heterogeneity of species that could be identified as factors influencing wildfire ignition. All studies cited in Table 2 and used as references to make comparisons with our study were selected regarding their core DL task, segmentation of forest point clouds, and their remote sensing data source; thus, studies that performed these types of forest analysis from 2D data were not considered.

González-Ferreiro et al. (2014) utilised geometric criteria to classify canopy forest point clouds according to their fuel type using low-density LiDAR data. However, the data used in their study was acquired from an ALS perspective, limiting the retrieval of fuel load information solely to the forest canopies. Conversely, the data collected for this study is TLS, which provides a wealth of information about the forests beneath the tree canopies. Consequently, a more accurate classification of the fuel model can be achieved by considering the vertical continuity criteria of the Prometheus model.

A recent study (Torresani et al., 2023) confirmed the height variation hypothesis, which predicts that high height heterogeneities in forest CHMs are a consequence of greater species diversity. The authors computed four different heterogeneity coefficients from two openly available CHMs and studied their linearity in the presence of the species. Furthermore, using similar sources, such as GEDI LiDAR, in combination with other remote sensing techniques, (Guo et al., 2023; Padalia et al., 2023)different methodologies have been proposed to retrieve the AGB in forested areas. Although in the present study, MS-TLS returns from the above tree canopies lacked reliability in dense forests, hindering the analysis of real tree heights, it offered a remarkable point of view from underneath tree canopies, offering a wider species diversity characterisation than that in Torresani et al. (2023). In addition, this characteristic of terrestrial measurements in combination with MS information

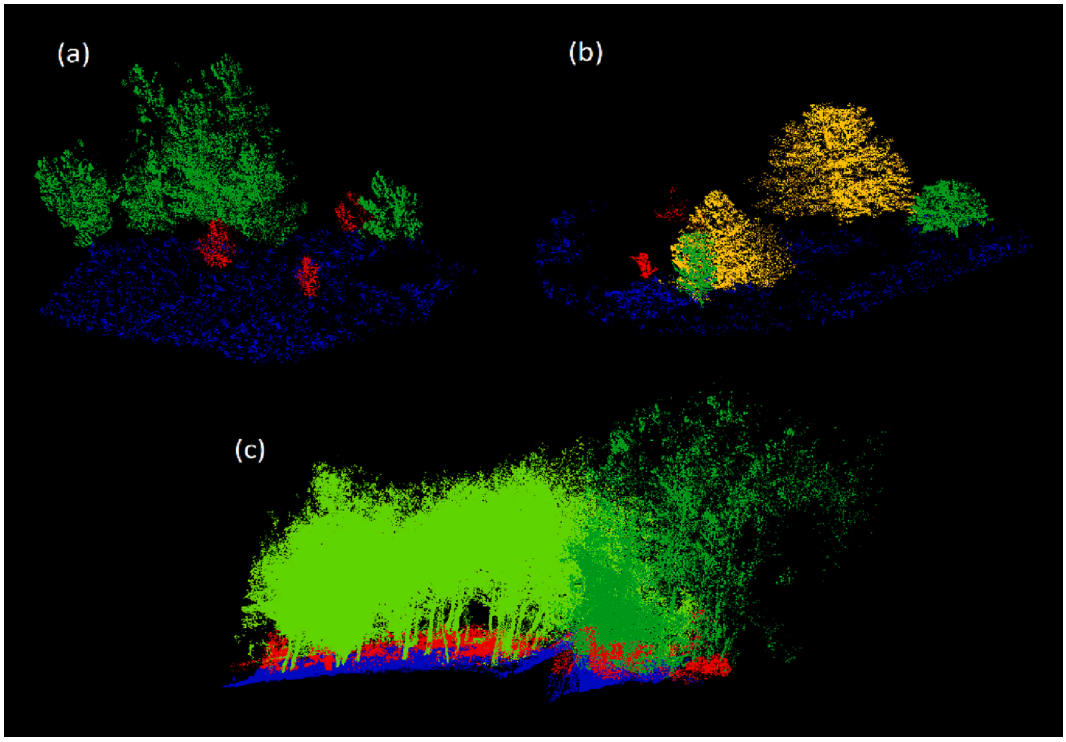


**Fig. 10.** Some examples of real MS point clouds segmented by the SoftGroup semantic branch. (a) Plot 1, (b) plot 2, and (c) plot 3. Blue: ground, dark green: fire-resistant, light green: fire-retardant, orange: fire-intolerant, and red: fine fuel. (For interpretation of the references to colour in this figure legend, the reader is referred to the web version of this article.)

enhances the existing analysis of AGB and the detection of potential wildfire triggers that are not visible from aerial and satellite perspectives.

Erdody and Moskal (2010) demonstrated that LiDAR properties outperformed spectral imagery in predicting canopy fuel metrics. Furthermore, combining 3D information with spectral imagery in the near-infrared range enhances the accuracy of the results, because spectral characteristics can differentiate vegetation elements. This concept was previously validated in this study, as evidenced by the results presented in Table 2, in which the forest inventory classification achieved superior metrics when the DL model incorporated one or more additional spectral kernels along with the raw geometry.

D'Este et al. (2021) employed various data sources to scan the fine dead fuel, and the authors successfully classified them using different machine learning algorithms. They concluded that variables related to vegetation structure play a crucial role in accurate fuel estimation, thereby increasing the relevance of using LiDAR data for fuel load estimation. By contrast, this study utilises a projection-based DL model, which offers distinct advantages over traditional machine learning methods. A DL model captures nonlinear relationships, automatically learns relevant features, and exhibits scalability. Additionally, a similar DL model framework allows for hierarchical representation and transfer learning capabilities.

Slightly different examples of DL applied within the context of fuel modelling can be found in Van Le et al. (2021) and Marjani et al. (2023), where the authors used different DL architectures to create forest fire susceptibility and propagation maps, respectively. These two types of maps were designed by considering four ignition factors that are well accepted in the literature and can be grouped into climatic, topographic, environmental, and anthropogenic factors. However, on one side, among environmental factors, those who directly face vegetation characteristics include only vegetation indices, such as the NDVI, NDWI and NDMI, and does not consider species diversities. This is also the case for works such as Bjånes et al. (2021) and Sivrikaya et al. (2024), where forest susceptibility to fire and wildfire risk maps were obtained, respectively, by considering most of the four ignition factors previously mentioned (Van Le et al., 2021), but not considering the intrinsic responses to fire of the different tree species and their horizontal and vertical distributions. However, in Van Le et al. (2021), it is stated that some variations in topographic factors can contribute to the generation of local climates, which can result in a greater species diversity; however, this is not considered to map the fire susceptibility. Conversely, as depicted in the current study and supported by Stefanidou et al. (2020), the surface fuel structure of vegetation can represent potential risks concerning the ignition of fire at different forest height levels, and species diversity can contribute to accelerating or decelerating the propagation of fire. This last affirmation is also supported by Blauw et al. (2017), who state that fire spread in forest plots differs depending on species abundance. For example, in the current study, plots 2, 4, 5, 7, and 8 were all classified as fuel type 5 by the geometrical criteria presented in Section 2.5; however, their species abundances were different, indicating that fire ignition and spread behave in different ways. In Botequim et al. (2019), the three types of fires considered by the authors were surface, passive, and active crown fires, and in 96–99% of observations, it was concluded that fire activity was rated as low in places mostly composed of pine species (surface fire). In addition, it was observed that in mixed forests composed of *Quercus* and *Pinus*, fire activity was higher (active crown fire). Both conclusions can be related to the plots classified as fuel type 5 in the current study, because they have different species abundances, and the fire should behave differently. According to their notation, plots 2, 4, 5, 7 and 8 can behave as surface and active crown fire models.

Finally, it is worth mentioning the recent methodology presented in Lin et al. (2024), which can be considered a 2D parallel case to the current study because different forest types are retrieved from semantic classifications of tree species within MS airborne imagery. Among the main contributions to the field, the results obtained from the selection of 72 spectral bands covering a wavelength range of 380–1050 nm

demonstrate the need to highlight the sensitivity of the models to band filtering. One of the TLS devices used in this study detects pulses at a wavelength of 1550 nm, which incorporates further insights into forest mapping regarding its species response to fire outside the spectral range analysed by Lin et al. (2024); this stands out from the rest of the state-of-the-art literature concerning forest fuel modelling.

As a conclusion for this section, it is necessary to highlight that the findings of this current study, whether concerning point-cloud simulation, applications of DL, or fuel modelling, carry significant ramifications in the ecological domain for forest management and conservation efforts.

## 5. Conclusions

A novel method was introduced to enhance the classification of fuel models using MS LiDAR data. This approach specifically targeted the assessment of fire responses in different forest types. The semantic branch of the advanced DL model SoftGroup was trained with synthetic data in different kernel configurations: raw geometry, spectral mono-bands, and MS, where the MS case achieved the best performance metrics.

Because this approach significantly reduces the time requirements, in this study, it was proven that the utilisation of synthetic forestry data within the DL framework is a valuable advantage, eliminating the need for manual labelling or relying on traditional machine learning approaches.

One of the outcomes of this study is the identification of more comprehensive fuel types in the Prometheus model, which conventionally considers only the structural information of trees and the understorey.

Given that existing fuel models solely account for structural information, this study emphasises the importance of incorporating semantic information into the flammability and fuel load of different vegetation species. Because conventional fuel schemes typically account solely for structural information, the addition of the proposed semantic information enhances the retrieval of fuel models in forest ecosystems and contributes to more effective wildfire management efforts, considering the varying behaviours of different vegetation species in response to fire. The methodology presented in this study can improve forest management practices and reduce the risk of catastrophic wildfires, making it a valuable tool for forest managers and fire management agencies.

## CRediT authorship contribution statement

**Lino Comesaña-Cebral:** Writing – original draft, Visualization, Validation, Software, Methodology, Formal analysis, Conceptualization. **Joaquín Martínez-Sánchez:** Writing – review & editing, Supervision. **Gabriel Suárez-Fernández:** Writing – review & editing, Resources. **Pedro Arias:** Writing – review & editing, Supervision, Conceptualization.

## Declaration of competing interest

The authors declare that they have no known competing financial interests or personal relationships that could have appeared to influence the work reported in this paper.

## Data availability

The data that has been used is confidential.

## Acknowledgments

This work was supported by the Spanish Government through the project 4Map4Health, selected in the call ERA-Net CHIST-ERA IV (2019), and founded by the State Research Agency of Spain (reference PCI2020-120705-2/AEI/10.13039/501100011033). We also acknowledge the funding by “Ayudas para la Formación de Profesorado Universitario (FPU)”, Ministry of Education, Government of Spain [FPU21/03038]. Funding for open access charge: Universidade de Vigo/CISUG. Simulations and Deep Learning derived results on this work were performed using the Finisterrae III Supercomputer, funded by the project CESGA-01 FINISTERRAE III.

## References

Abdollahi, A., Yebra, M., 2023. Forest fuel type classification: review of remote sensing techniques, constraints and future trends. J. Environ. Manag. 342, 118315 https://doi.org/10.1016/j.jenvman.2023.118315.

Alonso-Benito, A., Arroyo, L., Arbelo, M., Hernández-Leal, P., 2016. Fusion of WorldView-2 and LiDAR data to map fuel types in the Canary Islands. Remote Sens. 8 (8), 669. https://doi.org/10.3390/rs8080669.

Armeni, I., Sener, O., Zamir, A.R., Jiang, H., Brilakis, I., Fischer, M., Savarese, S., 2016. 3D semantic parsing of large-scale indoor spaces. In: 2016 IEEE Conference on Computer Vision and Pattern Recognition (CVPR), pp. 1534–1543. https://doi.org/10.1109/CVPR.2016.170.

Arroyo, L.A., Pascual, C., Manzanera, J.A., 2008. Fire models and methods to map fuel types: the role of remote sensing. For. Ecol. Manag. 256 (6), 1239–1252. https://doi.org/10.1016/j.foreco.2008.06.048.

Azizi, A., Mahboob, M., Monib, A.W., Hassand, M.H., Sediqi, S., Niazi, P., 2023. The role of plants in human health. Br. J. Biol. Stud. 3 (1), 08–12. https://doi.org/10.32996/bjbs.2023.3.1.2.

Baciu, G.E., Dobrotă, C.E., Apostol, E.N., 2021. Valuing forest ecosystem services. Why is an integrative approach needed? Forests 12 (6), 677. https://doi.org/10.3390/f12060677.

Bechtold, S., Höfle, B., 2016. Helios: A multi-purpose lidar simulation framework for research, planning and training of laser scanning operations with airborne, ground-based mobile and stationary platforms. In: ISPRS Annals of the Photogrammetry, Remote Sensing and Spatial Information Sciences, III–3, pp. 161–168. https://doi.org/10.5194/isprs-annals-III-3-161-2016.

Bjånes, A., De La Fuente, R., Mena, P., 2021. A deep learning ensemble model for wildfire susceptibility mapping. Eco. Inform. 65, 101397 https://doi.org/10.1016/j.ecoinf.2021.101397.

Blauw, L.G., van Logtestijn, R.S.P., Broekman, R., Aerts, R., Cornelissen, J.H.C., 2017. Tree species identity in high-latitude forests determines fire spread through fuel ladders from branches to soil and vice versa. For. Ecol. Manag. 400, 475–484. https://doi.org/10.1016/j.foreco.2017.06.023.

Botequim, B., Fernandes, P.M., Borges, J.G., González-Ferreiro, E., Guerra-Hernández, J., 2019. Improving silvicultural practices for Mediterranean forests through fire behaviour modelling using LiDAR-derived canopy fuel characteristics. Int. J. Wildland Fire 28 (11), 823. https://doi.org/10.1071/WF19001.

Bufacchi, P., Santos, J.C., de Carvalho, J.A., Krieger Filho, G.C., 2020. Estimation of the surface area-to-volume ratios of litter components of the Brazilian rainforest and their impact on litter fire rate of spread and flammability. J. Braz. Soc. Mech. Sci. Eng. 42 (5), 266. https://doi.org/10.1007/s40430-020-02303-8.

Cleve, C., Kelly, M., Kearns, F.R., Moritz, M., 2008. Classification of the wildland–urban interface: a comparison of pixel- and object-based classifications using high-resolution aerial photography. Comput. Environ. Urban. Syst. 32 (4), 317–326. https://doi.org/10.1016/j.compenvurbsys.2007.10.001.

Çolak, E., Sunar, F., 2020. Evaluation of forest fire risk in the Mediterranean Turkish forests: a case study of Menderes region, Izmir. Int. J. Disaster Risk Reduct. 45, 101479 https://doi.org/10.1016/j.ijdrr.2020.101479.

Comesaña Cebral, L.J., Martínez Sánchez, J., Rúa Fernández, E., Arias Sánchez, P., 2022. Heuristic generation of multispectral labeled point cloud datasets for deep learning models. In: The International Archives of the Photogrammetry, Remote Sensing and Spatial Information Sciences, XLIII-B2-2022, pp. 571–576. https://doi.org/10.5194/isprs-archives-XLIII-B2-2022-571-2022.

Comesaña-Cebral, L., Martínez-Sánchez, J., Lorenzo, H., Arias, P., 2021. Individual tree segmentation method based on mobile backpack LiDAR point clouds. Sensors 21 (18), 6007. https://doi.org/10.3390/s21186007.

Dai, A., Chang, A.X., Savva, M., Halber, M., Funkhouser, T., Nießner, M., 2017. ScanNet: Richly-Annotated 3D Reconstructions of Indoor Scenes.

Daşdemir, İ., Aydın, F., Ertuğrul, M., 2021. Factors affecting the behavior of large forest fires in Turkey. Environ. Manag. 67 (1), 162–175. https://doi.org/10.1007/s00267-020-01389-z.

D'Este, M., Elia, M., Giannico, V., Spano, G., Lafortezza, R., Sanesi, G., 2021. Machine learning techniques for fine dead fuel load estimation using multi-source remote sensing data. Remote Sens. 13 (9), 1658. https://doi.org/10.3390/rs13091658.

Dupire, S., Curt, T., Bigot, S., Fréjaville, T., 2019. Vulnerability of forest ecosystems to fire in the French Alps. Eur. J. For. Res. 138 (5), 813–830. https://doi.org/10.1007/s10342-019-01206-1.

Erdody, T.L., Moskal, L.M., 2010. Fusion of LiDAR and imagery for estimating forest canopy fuels. Remote Sens. Environ. 114 (4), 725–737. https://doi.org/10.1016/j.rse.2009.11.002.

Everingham, M., Eslami, S.M.A., Van Gool, L., Williams, C.K.I., Winn, J., Zisserman, A., 2015. The pascal visual object classes challenge: a retrospective. Int. J. Comput. Vis. 111 (1), 98–136. https://doi.org/10.1007/s11263-014-0733-5.

Ferster, C.J., Coops, N.C., 2016. Integrating volunteered smartphone data with multispectral remote sensing to estimate forest fuels. Int. J. Digit. Earth 9 (2), 171–196. https://doi.org/10.1080/17538947.2014.1002865.
Frejaville, T., Curt, T., Carcaillet, C., 2013. Bark flammability as a fire-response trait for subalpine trees. Front. Plant Sci. 4 https://doi.org/10.3389/fpls.2013.00466.
Fricker, G.A., Ventura, J.D., Wolf, J.A., North, M.P., Davis, F.W., Franklin, J., 2019. A convolutional neural network classifier identifies tree species in mixed-conifer forest from hyperspectral imagery. Remote Sens. 11 (19), 2326. https://doi.org/10.3390/rs11192326.
Geraskina, A.P., Tebenkova, D.N., Ershov, D.V., Ruchinskaya, E.V., Sibirtseva, N.V., Lukina, N.V., 2022. Wildfires as a factor of loss of biodiversity and forest ecosystem functions. For. Sci. Issues 5 (1), 1–70. https://doi.org/10.31509/2658-607x-202251-97.
González-Ferreiro, E., Diéguez-Aranda, U., Crecente-Campo, F., Barreiro-Fernández, L., Miranda, D., Castedo-Dorado, F., 2014. Modelling canopy fuel variables for Pinus radiata D. Don in NW Spain with low-density LiDAR data. Int. J. Wildland Fire 23 (3), 350. https://doi.org/10.1071/WF13054.
Guo, Y., Wang, H., Hu, Q., Liu, H., Liu, L., Bennamoun, M., 2021. Deep learning for 3D point clouds: a survey. IEEE Trans. Pattern Anal. Mach. Intell. 43 (12), 4338–4364. https://doi.org/10.1109/TPAMI.2020.3005434.
Guo, Q., Du, S., Jiang, J., Guo, W., Zhao, H., Yan, X., Zhao, Y., Xiao, W., 2023. Combining GEDI and sentinel data to estimate forest canopy mean height and aboveground biomass. Eco. Inform. 78, 102348 https://doi.org/10.1016/j.ecoinf.2023.102348.
Hamraz, H., Jacobs, N.B., Contreras, M.A., Clark, C.H., 2019. Deep learning for conifer/deciduous classification of airborne LiDAR 3D point clouds representing individual trees. ISPRS J. Photogramm. Remote Sens. 158, 219–230. https://doi.org/10.1016/j.isprsjprs.2019.10.011.
Hodge, R.A., 2010. Using simulated terrestrial laser scanning to analyse errors in high-resolution scan data of irregular surfaces. ISPRS J. Photogramm. Remote Sens. 65 (2), 227–240. https://doi.org/10.1016/j.isprsjprs.2010.01.001.
Hui, Z., Hu, Y., Yevenyo, Y., Yu, X., 2016. An improved morphological algorithm for filtering airborne LiDAR point cloud based on multi-level kriging interpolation. Remote Sens. 8 (1), 35. https://doi.org/10.3390/rs8010035.
Kaijaluoto, R., Kukko, A., El Issaoui, A., Hyyppä, J., Kaartinen, H., 2022. Semantic segmentation of point cloud data using raw laser scanner measurements and deep neural networks. ISPRS Open J. Photogram. Remote Sens. 3, 100011 https://doi.org/10.1016/j.ophoto.2021.100011.
Kalinaki, K., Malik, O.A., Lai, D.T.C., Sukri, R.S., Wahab, R.B.H.A., 2023. Spatial-temporal mapping of forest vegetation cover changes along highways in Brunei using deep learning techniques and Sentinel-2 images. Eco. Inform. 77, 102193 https://doi.org/10.1016/j.ecoinf.2023.102193.
Kim, S., Min, S., Kim, G., Lee, I., Jun, C., 2009. In: Turner, M.D., Kamerman, G.W. (Eds.), Data simulation of an airborne lidar system, p. 73230C. https://doi.org/10.1117/12.818545.
Kukko, A., Hyyppä, J., 2009. Small-footprint laser scanning simulator for system validation, error assessment, and algorithm development. Photogramm. Eng. Remote. Sens. 75 (10), 1177–1189. https://doi.org/10.14358/PERS.75.10.1177.
Labenski, P., Ewald, M., Schmidtlein, S., Fassnacht, F.E., 2022. Classifying surface fuel types based on forest stand photographs and satellite time series using deep learning. Int. J. Appl. Earth Obs. Geoinf. 109, 102799 https://doi.org/10.1016/j.jag.2022.102799.
Lavalle, M., Khun, K., 2014. Three-baseline InSAR estimation of forest height. IEEE Geosci. Remote Sens. Lett. 11 (10), 1737–1741. https://doi.org/10.1109/LGRS.2014.2307583.
Lian, X., Zhang, H., Xiao, W., Lei, Y., Ge, L., Qin, K., He, Y., Dong, Q., Li, L., Han, Y., Fan, H., Li, Y., Shi, L., Chang, J., 2022. Biomass calculations of individual trees based on unmanned aerial vehicle multispectral imagery and laser scanning combined with terrestrial laser scanning in complex stands. Remote Sens. 14 (19) https://doi.org/10.3390/rs14194715.
Lin, F.-C., Shiu, Y.-S., Wang, P.-J., Wang, U.-H., Lai, J.-S., Chuang, Y.-C., 2024. A model for forest type identification and forest regeneration monitoring based on deep learning and hyperspectral imagery. Eco. Inform. 80, 102507 https://doi.org/10.1016/j.ecoinf.2024.102507.
Marino, E., Ranz, P., Tomé, J.L., Noriega, M.Á., Esteban, J., Madrigal, J., 2016. Generation of high-resolution fuel model maps from discrete airborne laser scanner and Landsat-8 OLI: a low-cost and highly updated methodology for large areas. Remote Sens. Environ. 187, 267–280. https://doi.org/10.1016/j.rse.2016.10.020.
Marjani, M., Ahmadi, S.A., Mahdianpari, M., 2023. FirePred: a hybrid multi-temporal convolutional neural network model for wildfire spread prediction. Eco. Inform. 78, 102282 https://doi.org/10.1016/j.ecoinf.2023.102282.
Mihajlovski, B., Fernandes, P.M., Pereira, J.M.C., Guerra-Hernández, J., 2023. Comparing forest understory fuel classification in Portugal using discrete airborne laser scanning data and satellite multi-source remote sensing data. Fire 6 (9). https://doi.org/10.3390/fire6090327.
Mutlu, M., Popescu, S., Stripling, C., Spencer, T., 2008. Mapping surface fuel models using lidar and multispectral data fusion for fire behavior. Remote Sens. Environ. 112 (1), 274–285. https://doi.org/10.1016/j.rse.2007.05.005.
Novo, A., Fariñas-Álvarez, N., Martínez-Sánchez, J., González-Jorge, H., Lorenzo, H., 2020. Automatic processing of aerial LiDAR data to detect vegetation continuity in the surroundings of roads. Remote Sens. 12 (10), 1677. https://doi.org/10.3390/rs12101677.
Padalia, H., Prakash, A., Watham, T., 2023. Modelling aboveground biomass of a multistage managed forest through synergistic use of Landsat-OLI, ALOS-2 L-band SAR and GEDI metrics. Eco. Inform. 77, 102234 https://doi.org/10.1016/j.ecoinf.2023.102234.
Qi, C.R., Yi, L., Su, H., Guibas, L.J., 2017. PointNet++: Deep Hierarchical Feature Learning on Point Sets in a Metric Space.
Ramakrishnan, P.S., 2007. Traditional forest knowledge and sustainable forestry: a north-East India perspective. For. Ecol. Manag. 249 (1–2), 91–99. https://doi.org/10.1016/j.foreco.2007.04.001.
Riaño, D., Chuvieco, E., Salas, J., Palacios-Orueta, A., Bastarrika, A., 2002. Generation of fuel type maps from Landsat TM images and ancillary data in Mediterranean ecosystems. Can. J. For. Res. 32 (8), 1301–1315. https://doi.org/10.1139/x02-052.
Richardson, D.M., Cowling, R.M., Le Maitre, D.C., 1990. Assessing the risk of invasive success in Pinus and Banksia in south African mountain fynbos. J. Veg. Sci. 1 (5), 629–642. https://doi.org/10.2307/3235569.
RIEGL miniVUX-1DL data sheet, 2020, March 26. https://www.gtbi.net/wp-content/uploads/2021/06/riegl-minivux-1dl_folleto(EN).pdf.
RIEGL VUX-1UAV Data Sheet, 2020, September 22. http://www.riegl.com/products/unmanned-scanning/riegl-vux-1uav22/.
Sharma, N., Sharma, R., Jindal, N., 2021. Machine learning and deep learning applications-a vision. Glob. Trans. Proc. 2 (1), 24–28. https://doi.org/10.1016/j.gltp.2021.01.004.
Sivrikaya, F., Günlü, A., Küçük, Ö., Ürker, O., 2024. Forest fire risk mapping with Landsat 8 OLI images: evaluation of the potential use of vegetation indices. Eco. Inform. 79, 102461 https://doi.org/10.1016/j.ecoinf.2024.102461.
Skowronski, N., Clark, K., Nelson, R., Hom, J., Patterson, M., 2007. Remotely sensed measurements of forest structure and fuel loads in the Pinelands of New Jersey. Remote Sens. Environ. 108 (2), 123–129. https://doi.org/10.1016/j.rse.2006.09.032.
Stefanidou, A., Z Gitas, I., Korhonen, L., Georgopoulos, N., Stavrakoudis, D., 2020. Multispectral LiDAR-based estimation of surface fuel load in a dense coniferous forest. Remote Sens. 12 (20), 3333. https://doi.org/10.3390/rs12203333.
Sullivan, T.P., Sullivan, D.S., 2016. Wildfire, clearcutting, and vole populations: balancing forest crop protection and biodiversity. Crop Prot. 85, 9–16. https://doi.org/10.1016/j.cropro.2016.03.012.
Tinner, W., Conedera, M., Gobet, E., Hubschmid, P., Wehrli, M., Ammann, B., 2000. A palaeoecological attempt to classify fire sensitivity of trees in the southern Alps. The Holocene 10 (5), 565–574. https://doi.org/10.1191/095968300674242447.
Torresani, M., Rocchini, D., Alberti, A., Moudrý, V., Heym, M., Thouverai, E., Kacic, P., Tomelleri, E., 2023. LiDAR GEDI derived tree canopy height heterogeneity reveals patterns of biodiversity in forest ecosystems. Eco. Inform. 76, 102082 https://doi.org/10.1016/j.ecoinf.2023.102082.
Van Le, H., Hoang, D.A., Tran, C.T., Nguyen, P.Q., Tran, V.H.T., Hoang, N.D., Amiri, M., Ngo, T.P.T., Nhu, H.V., Van Hoang, T., Tien Bui, D., 2021. A new approach of deep neural computing for spatial prediction of wildfire danger at tropical climate areas. Eco. Inform. 63, 101300 https://doi.org/10.1016/j.ecoinf.2021.101300.
Vu, T., Kim, K., Luu, T.M., Nguyen, T., Kim, J., Yoo, C.D., 2022a. Scalable SoftGroup for 3D Instance Segmentation on Point Clouds.
Vu, T., Kim, K., Luu, T.M., Nguyen, X.T., Yoo, C.D., 2022b. SoftGroup for 3D Instance Segmentation on Point Clouds.
Wang, Y., Xie, D., Yan, G., Zhang, W., Mu, X., 2013. Analysis on the inversion accuracy of LAI based on simulated point clouds of terrestrial LiDAR of tree by ray tracing algorithm. In: 2013 IEEE International Geoscience and Remote Sensing Symposium - IGARSS, pp. 532–535. https://doi.org/10.1109/IGARSS.2013.6721210.
Wang, B.H., Diaz-Ruiz, C., Banfi, J., Campbell, M., 2021. Detecting and mapping trees in unstructured environments with a stereo camera and pseudo-lidar. In: 2021 IEEE International Conference on Robotics and Automation (ICRA), pp. 14120–14126. https://doi.org/10.1109/ICRA48506.2021.9562056.
Wang, Z., Li, P., Cui, Y., Lei, S., Kang, Z., 2023. Automatic detection of individual trees in forests based on airborne LiDAR data with a tree region-based convolutional neural network (RCNN). Remote Sens. 15 (4), 1024. https://doi.org/10.3390/rs15041024.
Winiwarter, L., Esmorís Pena, A.M., Weiser, H., Anders, K., Martínez Sánchez, J., Searle, M., Höfle, B., 2022. Virtual laser scanning with HELIOS++: a novel take on ray tracing-based simulation of topographic full-waveform 3D laser scanning. Remote Sens. Environ. 269, 112772 https://doi.org/10.1016/J.RSE.2021.112772.
Xi, Z., Hopkinson, C., Rood, S.B., Peddle, D.R., 2020. See the forest and the trees: effective machine and deep learning algorithms for wood filtering and tree species classification from terrestrial laser scanning. ISPRS J. Photogramm. Remote Sens. 168, 1–16. https://doi.org/10.1016/j.isprsjprs.2020.08.001.
Xu, Y., Li, D., Ma, H., Lin, R., Zhang, F., 2022. Modeling Forest fire spread using machine learning-based cellular automata in a GIS environment. Forests 13 (12), 1974. https://doi.org/10.3390/f13121974.
Zhang, W., Qi, J., Wan, P., Wang, H., Xie, D., Wang, X., Yan, G., 2016. An easy-to-use airborne LiDAR data filtering method based on cloth simulation. Remote Sens. 8 (6), 501. https://doi.org/10.3390/rs8060501.